catalysts

Supplementary Materials

Microwave-induced deep oxidation of brilliant green using carbon nanotube-supported bismuth ferrite

Haoran liu [1], Hongzhe Chen [2], Yan Xue [3], Qiang Zhong [3,4]* and Shaogui Yang [3]

[1] Department of Chemistry, University of Liverpool, Liverpool, L69 7ZX, UK
[2] Third Institute of Oceanography, Ministry of Natural Resources, No. 178, Daxue Road, Siming District, Xiamen, 361005, P.R. China
[3] School of Environment, Jiangsu Province Engineering Research Center of Environmental Risk Prevention and Emergency Response Technology, Jiangsu Engineering Lab of Water and Soil Eco-remediation, Nanjing Normal University, No. 1 Wen yuan Road, Nanjing, Jiangsu 210023, P.R. China.
[4] School of Geography, Nanjing Normal University, Nanjing, Jiangsu 210023, P.R. China.

Text

Text S1 Pretreatment process for GCMS

The pretreatment process was as follows: 15 mL of filtered solution was extracted three times, using 25 mL of n-hexane, and the extracted solution was dehydrated using anhydrous sodium sulfate. Afterward, the dehydrated solution was concentrated to 1 mL and blown dry with a nitrogen evaporator. Before GC-MS analysis, trimethylsilylating derivatization was carried out at 323 K for 30 min using 0.5 mL of bis(trimethylsilyl)trifluoroacetamide (BSTFA). The final sample (2.0 μL) was automatically injected into a GC with a DB-5 column with the splitless mode. The oven temperature was programmed as follows: the initial temperature was 313 K; then, it rose to 523 K at a ramping rate of 5 K min^{-1}; after holding 2 min, it rose to 553 K at a ramping rate of 10 K min^{-1}, and held for another 2 min. The MS was operated in the 70 eV electron impact (EI) mode and positive ion mode.

Table S1. Concentration of Fe^{2+}/Fe^{3+} leaching from BFNT into solution after the MW-induced reaction (10 min radiation, BFNTs with CNTs at a mass ratio of 10%).

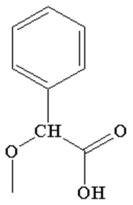
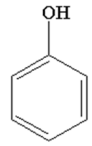
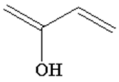
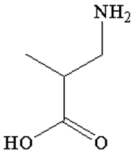
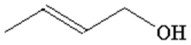
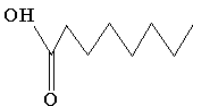
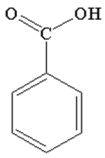
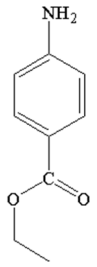
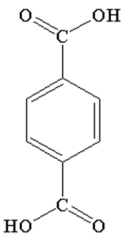
Group	Concentration (mg/L)
Control	0.008±0.001
Degradation	0.008±0.001
After regeneration	0.004±0.001

Copyright: © 2025 by the authors. Licensee MDPI, Basel, Switzerland. This article is an open access article distributed under the terms and conditions of the Creative Commons Attribution (CC BY) license (https://creativecommons.org/licenses/by/4.0/).

Table S2. Complex electromagnetic parameters of BFO and BFNTs at 2.45 GHz frequency of microwave radiation. Here, ε' is a dielectric constant and ε'' is a dielectric loss factor.

Absorbent	ε'	ε''	μ'	μ''	Dielectric loss tangents (rad) $= \frac{\varepsilon''}{\varepsilon'}$	Magnetic factor loss (rad) $= \frac{\mu''}{\mu'}$
BFO	6.546	0.255	1.208	0.150	0.039	0.124
BFNTs	7.428	0.323	1.245	0.163	0.043	0.131

Table S3. Main products identified by GC–EI-MS (identified with NIST library).

Intermediates	Derivatives' t_R (min)	m/z	Derivatives' fragments (m/z, %)
	5.84	166	73 (85), 121 (100), 221 (45)
	5.9	94	151 (100), 166 (25)
	6.73	70	73 (100), 127 (73), 215 (75)
	7.86	103	73 (100), 130 (45), 174 (30), 202 (25)
	8.13	72	73 (100), 144 (23)
	8.20	144	73 (100), 117 (48), 201 (55)
	8.75	122	77 (55), 105 (73); 135 (50); 179 (100)
	12.35	165	73 (27), 149 (30), 192 (40), 222 (100), 237 (85)
	14.93	166	73 (25), 103 (20), 221 (25), 295 (100)

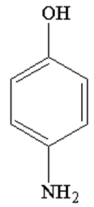
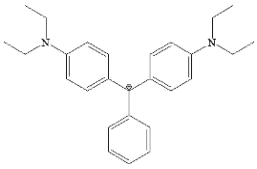
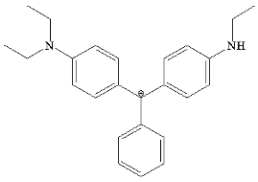
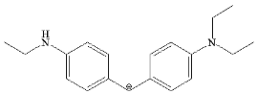
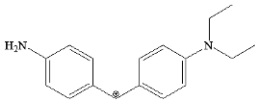
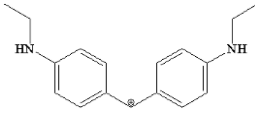
	17.3	228	73 (100), 117 (60), 132 (30), 145 (20)
	22.78	109	77 (25), 105 (30), 149 (20), 238 (100), 253 (45)

Table S4. Main products identified by LC–ESI-MS (proven by standard).

Intermediates	Derivatives' t_R (min)	m/z (scanning mode)	Derivatives' fragments (m/z)
	32.44	385 (+)	385.4
	39.67	357 (+)	313.3, 357.2
	41.08	281 (+)	254.1, 267.4, 281.2
	34.35	254 (+)	105.1, 225.1
	47.01	254 (+)	224.1

Figure

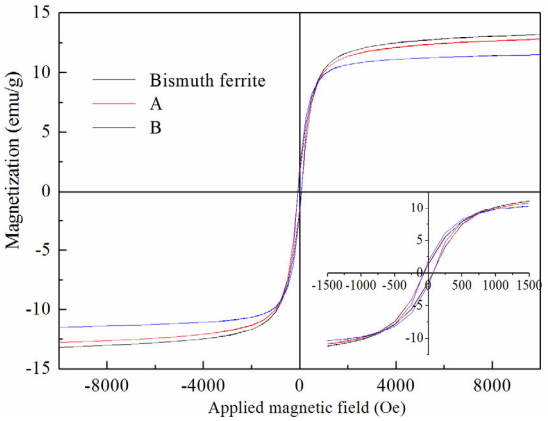


Figure S1. M-H hysteresis loops of BFO nanoparticles; (A) BFNTs with CNTs with a mass ratio of 10%; (B) BFNTs with CNTs with a mass ratio of 40%. (Measured at 300 K; the partially enlarged curve is the inset).

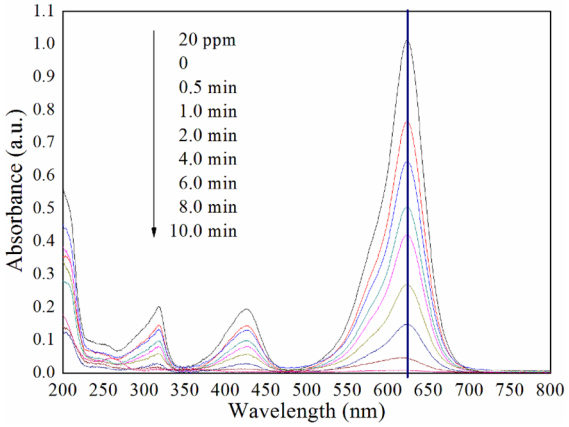


Figure S2. UV–Vis spectral variation of aqueous solution of BG dye in the presence of BFNTs with CNTs with a mass ratio of 10% at different MW reaction times.

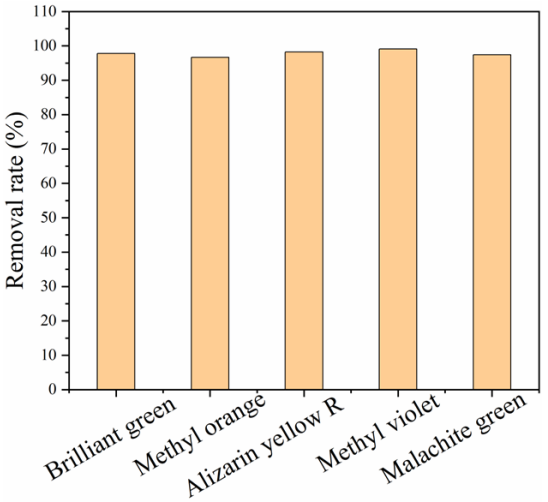


Figure S3. Temporal course of the MW-induced degradation of different pollutants in the presence of 20-BFNTs.

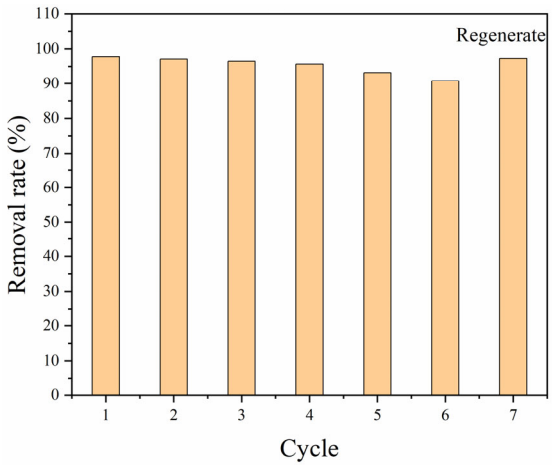


Figure S4. Reusability of catalysts.

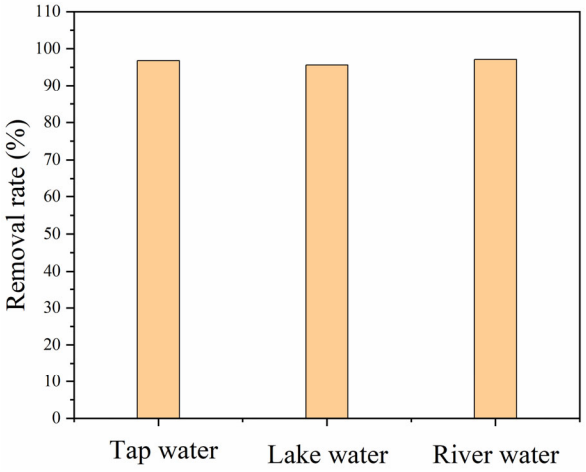


Figure S5. BG removal rate in different sources of water.

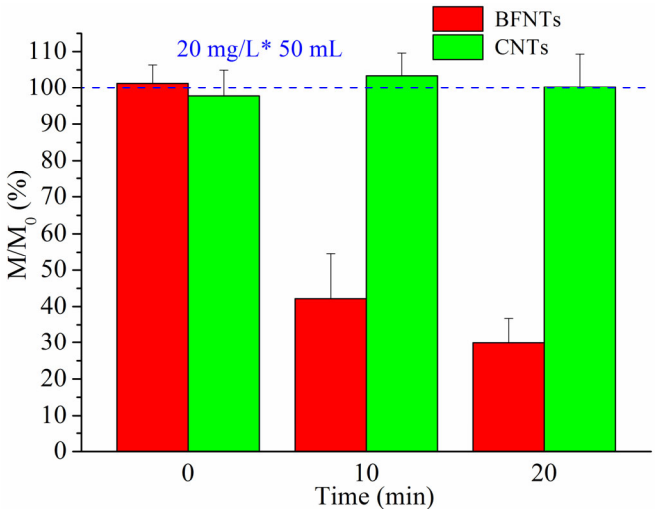


Figure S6. MW-induced degradation course of adsorbed BG over BFNTs with CNTs at the ratio of 40%, as well as CNTs. The blue dashed line represents the calculated mass ratio of BG corresponding to 20 mg/L in aqueous solution, namely 100%.

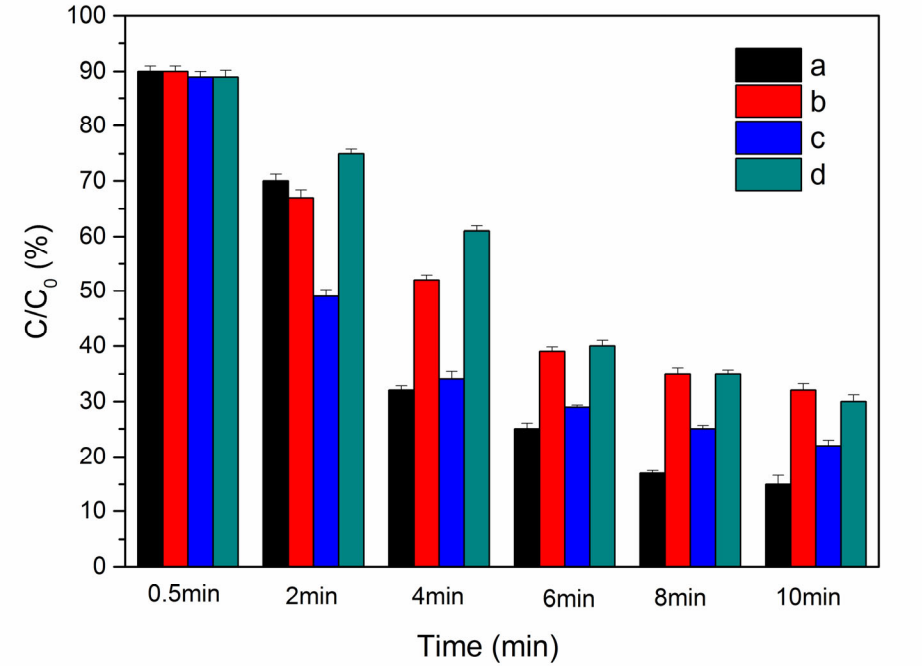


Figure S7. MW-induced degradation course of BG over BFO (a, b) and BFNTs with CNTs at the ratio of 10% (c, d). Superoxide radical scavenger was also added (b, d).

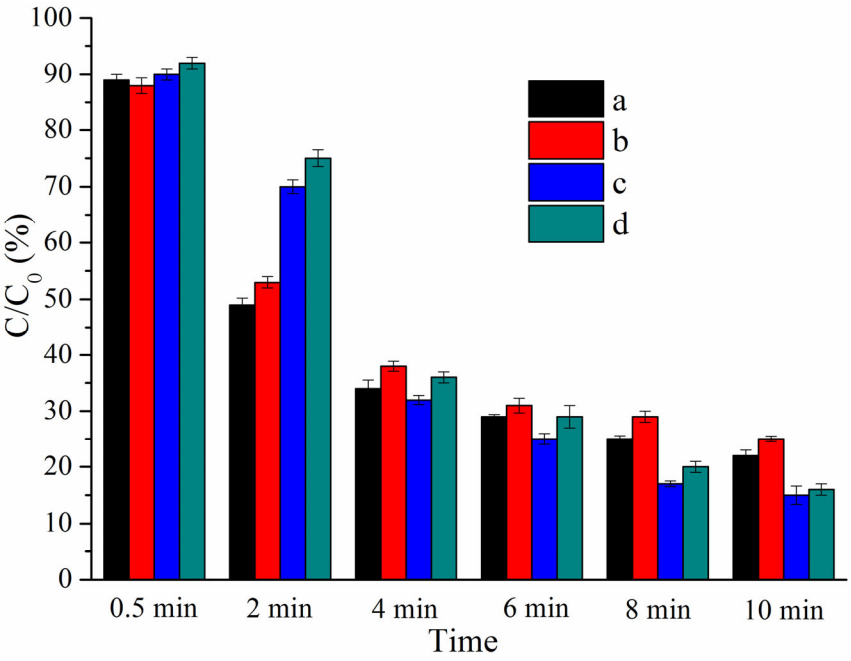


Figure S8. MW-induced degradation course of BG over BFO (a, b) and BFNTs with CNTs at the ratio of 10% (c, d). Hydroxyl radical scavenger was also added (b, d).

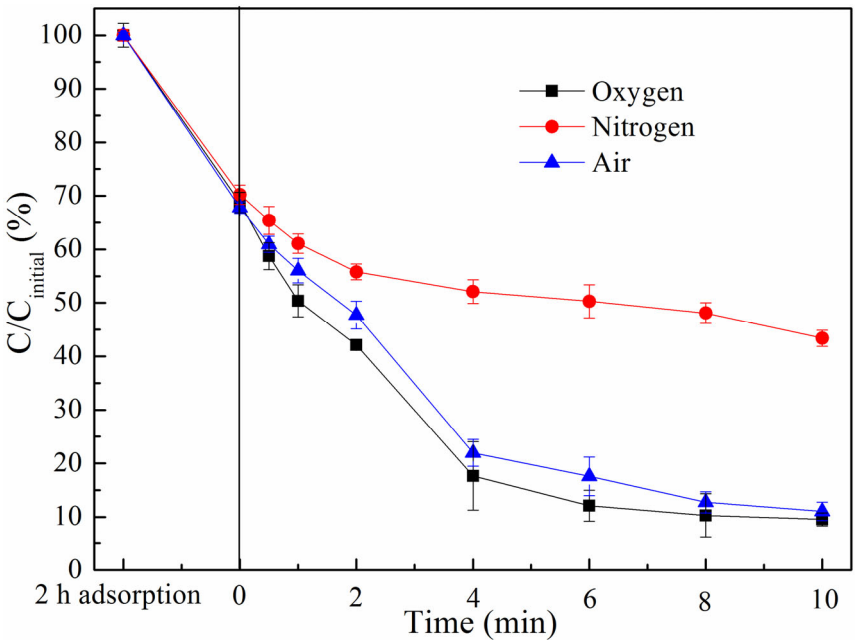


Figure S9. MW-induced degradation course of BG in the presence of BFNTs with CNTs at the ratio of 10%, where oxygen, nitrogen, or compressed air was pumped into the reactor (1 mL min^{-1}).

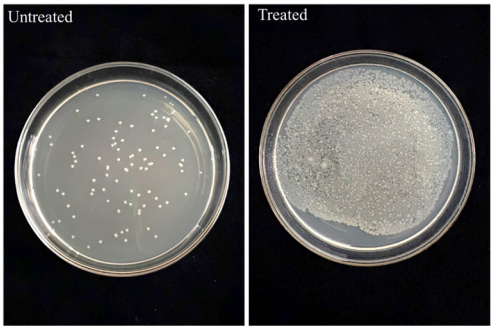


Figure S10. Photographs of E. coli colonies cultured in solution-treated and untreated systems.



Figure S11. Physical object image of the MW oven.

Scheme

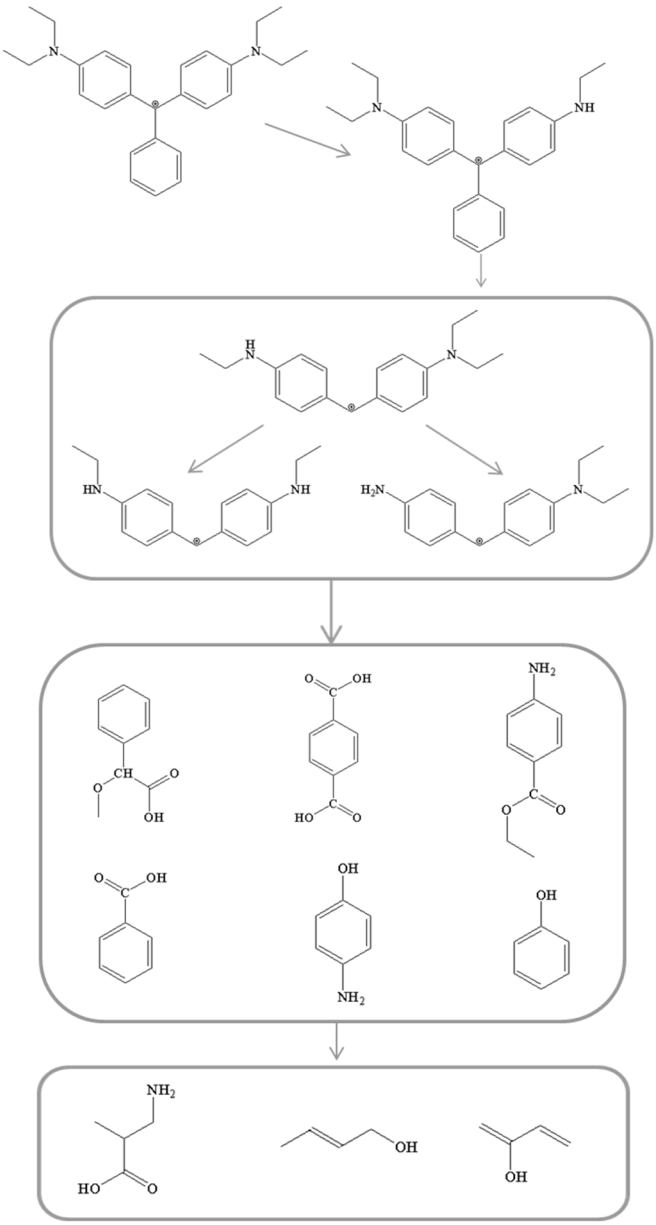
$$BFNTs + energy \rightarrow h^{*+} + e^{*-}$$

$$h^{*+} + organic \rightarrow products$$

$$e^{*-} + O_2 \rightarrow O_2^{*-}$$

$$O_2^{*-} + organic \rightarrow products$$

Scheme 1. The proposed mechanism of MW induced degradation course of BG.



Scheme 2. The proposed degradation pathways of BG in the presence of BFNTs with CNTs at the ratio of 10%.

Disclaimer/Publisher's Note: The statements, opinions and data contained in all publications are solely those of the individual author(s) and contributor(s) and not of MDPI and/or the editor(s). MDPI and/or the editor(s) disclaim responsibility for any injury to people or property resulting from any ideas, methods, instructions or products referred to in the content.